Applied Surface Science 669 (2024) 160475

Contents lists available at ScienceDirect

Applied Surface Science

journal homepage: www.elsevier.com/locate/apsusc

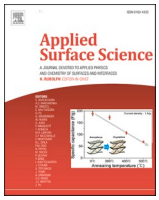

Full Length Article

# Dissociative adsorption of supersonic $CH_3Cl$ on Cu oxide Surfaces: $Cu_2O$ (111) and bulk $Cu_2O$ precursor "29"-Structure on Cu(111)

Koki Hayashida [a], Yasutaka Tsuda [b], Natsumi Murase [a], Takashi Yamada [a], Akitaka Yoshigoe [b], Wilson Agerico Diño [c], Michio Okada [a,d,*]

[a] Department of Chemistry, Graduate School of Science, The University of Osaka, Toyonaka, Osaka 560-0043, Japan
[b] Materials Sciences Research Center, Japan Atomic Energy Agency, Sayo-gun, Hyogo 679-5148, Japan
[c] Department of Applied Physics, The University of Osaka, Suita, Osaka 565-0871, Japan
[d] Institute of Radiation Sciences, The University of Osaka, Toyonaka, Osaka 560-0043, Japan

A B S T R A C T

To examine the elementary steps of the Rochow-Müller process we placed copper oxides, viz., $Cu_2O$(111) and the bulk $Cu_2O$ precursor "29"-structure on Cu(111), under supersonic molecular beams (SSMB) of $CH_3Cl$. The SSMB energies range from 0.5-1.9 eV. We employed X-ray photoemission spectroscopy (XPS) in conjunction with synchrotron radiation (SR) to determine the resulting adsorbed species present. We identified two reaction paths, viz., Reaction I and Reaction II. Reaction I involves dissociative adsorption of $CH_3Cl$. In Reaction II, $CH_3Cl$ also dissociates, but with Cl as the dominant adsorbed species (higher than that of adsorbed carbonaceous species, as observed for Reaction I). For the incident energies and exposure conditions considered, we found Reaction II as the dominant reaction path for $CH_3Cl$ reaction on both $Cu_2O$(111) and the "29"-structure on Cu(111).

## 1. Introduction

The discovery of the Rochow-Müller process in 1945 served as a breakthrough for the silicone industry [1–4]. With the aid of copper-based catalyst, this simple (to implement) but highly selective process allows for the industrial-scale production of dimethyldichlorosilane ($(CH_3)_2SiCl_2$, M2), the principal precursor to silicone compounds [1–4]. Despite experimental and theoretical efforts (cf., e.g., [3–19] and references therein), a clear understanding of the many-body Rochow-Müller process has remained elusive, esp., the actual form and role of the Cu(-based) catalyst. For example, previous studies report that $CH_3Cl$ dissociatively adsorbs (cf., e.g., [15] and references therein) on the low-index surfaces of $Cu_2O$, a *p*-type semiconductor with a band gap of ca. 2.1 eV [20]. $CH_3$ bond to surface O and Cl bonds to surface Cu of $Cu_2O$ [15]. On pure Cu surfaces, previous studies report that $CH_3Cl$ also dissociates [14]. However, only Cl adsorbs on the pure Cu surface. The $CH_3$ scatters back to the vacuum [14].

Here, we report on the reaction of energetic $CH_3Cl$ with copper oxide surfaces, viz., $Cu_2O$(111) and the bulk $Cu_2O$ precursor "29"-structure on Cu(111) (so named because the oxide layer has a unit cell area 29 times that of the underlying Cu(111) unit cell, cf., e.g., [20] and references therein). We bombarded the copper oxide surfaces with supersonic (ca. 0.5 ~ 1.9 eV) molecular beams (SSMB) of $CH_3Cl$. We then determined the resulting adsorbed species present on the surface using X-ray photoemission spectroscopy (XPS), in conjunction with synchrotron radiation (SR). We were able to identify two competing reaction paths. One results in the dissociative adsorption of $CH_3Cl$ (Reaction I), and the other results in the adsorption of Cl and scattering of $CH_3$ (Reaction II). One reaction process dominates over the other depending on the $CH_3Cl$ incident energy. These results hint at the role of copper oxides in realizing the high efficiency and high selectivity of the Rochow-Müller process.

## 2. Experimental methodology

We carried out all the experiments with the surface reaction analysis apparatus (SUREAC 2000) built at BL23SU in the third-generation synchrotron radiation facility of SPring-8 [21–25]. Briefly, SUREAC2000 has a base pressure of $< 2 \times 10^{-8}$ Pa, a photo-electron energy analyzer (OMICRON EA125-5MCD) and a Mg/Al Kα twin anode X-ray source (OMICRON DAR400). It is also equipped with a quadrupole mass spectrometer, located opposite the $CH_3Cl$ SSMB source, for monitoring the molecular beam. To generate 0.5 ~ 1.9 eV $CH_3Cl$ SSMB, we employed the adiabatic expansion of a gas mixture of $CH_3Cl$ and He from a nozzle with a small orifice at 300 ~ 773 K. To clean the bulk $Cu_2O$(111) (purchased from SurfaceNet GmbH) samples (10

* Corresponding author.
*E-mail address:* okada@chem.sci.osaka-u.ac.jp (M. Okada).

https://doi.org/10.1016/j.apsusc.2024.160475
Received 5 April 2024; Received in revised form 18 May 2024; Accepted 3 June 2024
Available online 4 June 2024

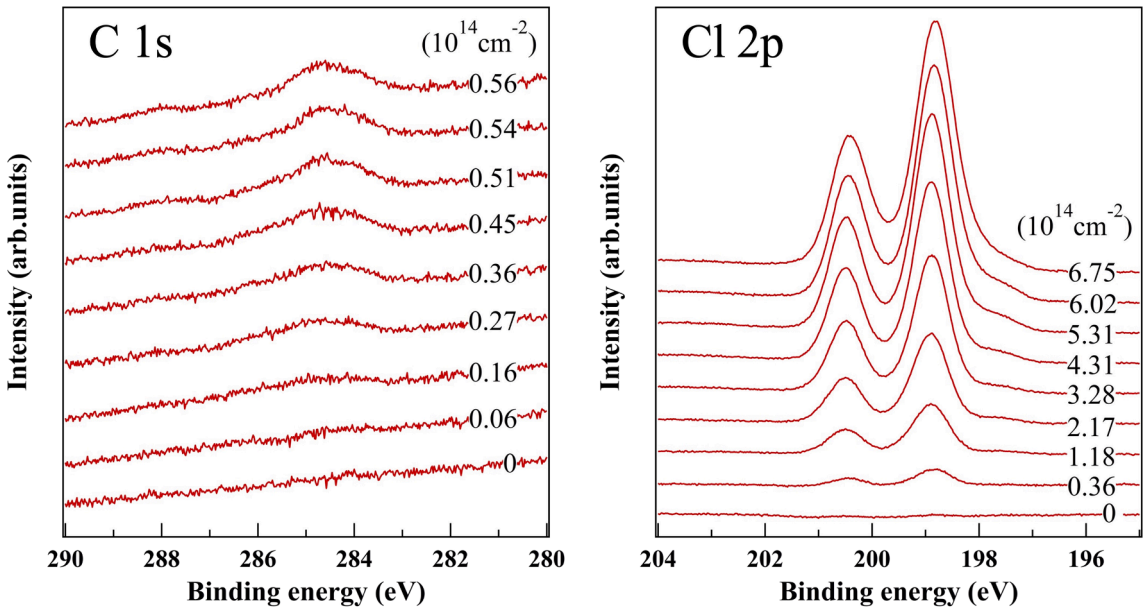


**Fig. 1.** Evolution of typical XPS spectra of C-1*s* and Cl-2*p* measured after the energetic 1.2 eV $CH_3Cl$ incidence on $Cu_2O(111)$ at 300 K.

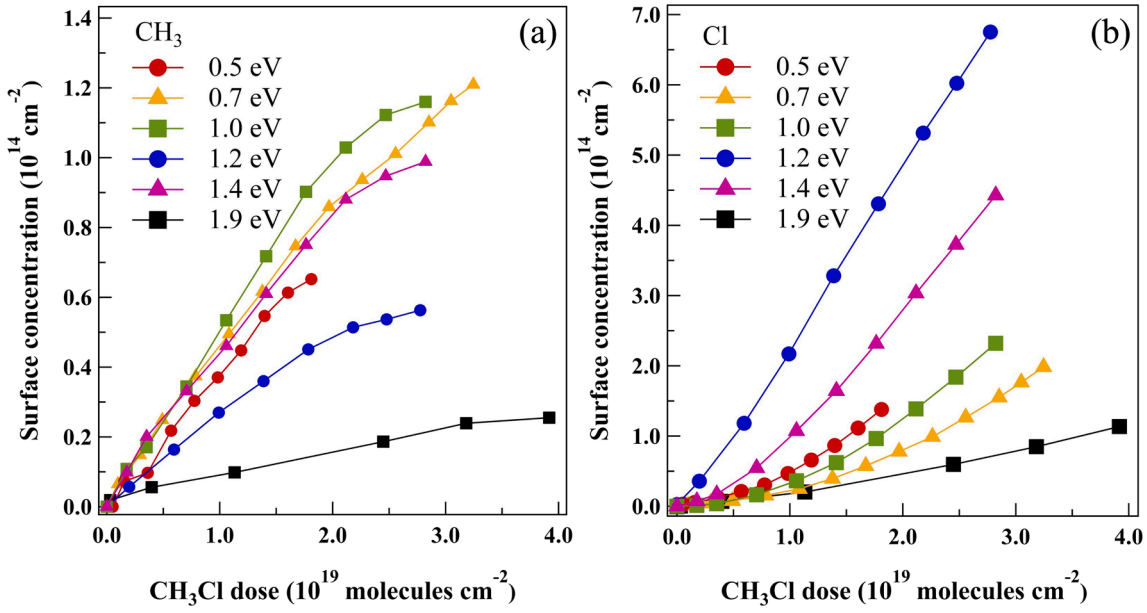


**Fig. 2.** (a) $CH_3$ and (b) Cl uptake curves for $CH_3Cl$ at various incident translational energies on $Cu_2O(111)$.

mm × 10 mm × 1 mm), we repeatedly sputter (with 1.5 keV $Ar^+$) and anneal (for 20 min at 723 ~ 773 K) the sample until no impurities were detectable by synchrotron-radiation XPS (SR-XPS). The low-energy electron diffraction (LEED) of the prepared clean $Cu_2O(111)$ surface shows the $(\sqrt{3} \times \sqrt{3})R30^\circ$ (Supplementary Data 1: Fig. 1S). For the bulk $Cu_2O$ precursor "29" structure on Cu(111), we prepared a thin oxide layer on the clean Cu(111) as we reported in [20]. (A typical LEED pattern, the O-1*s* spectrum and the corresponding structural model of "29" structure is shown in Supplementary Data 2: Fig. 2S.) We irradiated the clean copper oxide surfaces (viz., $Cu_2O(111)$ and the "29" structure) with varying SSMBs incident energies. We then characterized the resulting surfaces by performing SR-XPS measurements (at 300 K) with 741 eV soft X-ray photons. The high-intensity focused X-ray beam allowed for short (time period) but highly-resolved XPS spectra measurements with reasonably high S/N ratios and fine-peak deconvolution. The pass energy of the photo-electrons in the energy analyzer was set to 10 eV. To calculate the area intensities for the evaluation of the surface reactivity, we subtracted the background from the SR-XPS measured C-1*s* and Cl-2*p* (using the Shirley method [26] for the Cl-2*p* spectra and linear background subtraction for the C-1*s* spectra), and then, integrated the resulting peaks.

## 3. Results and discussions

Fig. 1 shows typical C-1*s* and Cl-2*p* XPS spectra measured after exposure of $Cu_2O(111)$ to 1.2 eV $CH_3Cl$ at $T_S$ = 300 K (cf., Supplementary Data 3: Fig. 3S for XPS spectra for the other incident energies). Cl-2*p* spectra show a clear peak growth with increasing $CH_3Cl$ dose, whereas the C-1*s* spectra show broader and less prominent peak growth. In Fig. 2, we show the measured incident-energy dependent uptake curves for the dissociative adsorption of $CH_3Cl$ on $Cu_2O(111)$ at $T_S$ =

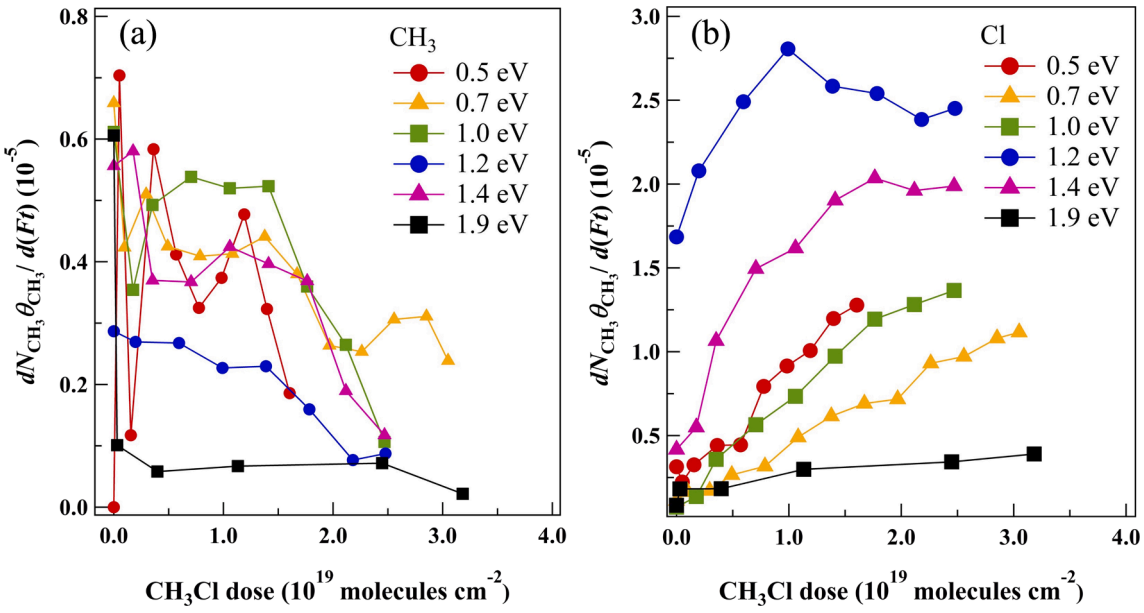


**Fig. 3.** Reaction rates determined from the slope of the (a) $CH_3$ and (b) Cl uptake curves (Fig. 2).

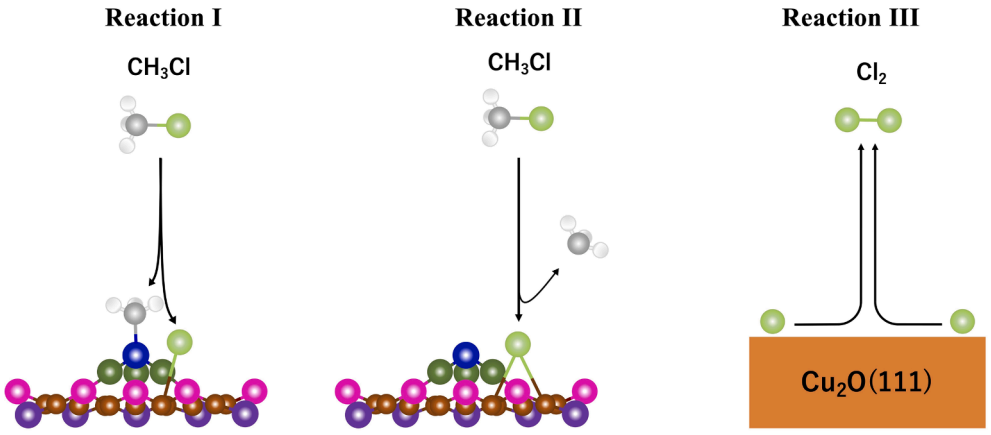


**Fig. 4.** Some depictions of possible $CH_3Cl$ reaction processes on $Cu_2O(111)$ viz., Reaction I: dissociative adsorption, Reaction II: abstractive reaction (dissociative scattering and adsorption), and Reaction III: associative desorption.

300 K. We obtained the uptake curves by integrating the C-1*s* and Cl-2*p* spectra in Fig. 1 (cf., Supplementary Data 3: Fig. 3S). We see that the C and Cl uptake curves follow different trends. At the same exposure (fixed $CH_3Cl$ dose), the $CH_3$ and Cl coverages reach maxima at $E_i = 1.0$ and 1.2 eV, respectively. The $CH_3$ uptake curves show no clear incident energy dependence (except for the outlying $E_i = 1.2$ and 1.9 eV at high $CH_3Cl$ dose), in contrast to that of Cl uptake curve. At $E_i = 1.2$ eV, although the Cl adsorption increases with $CH_3Cl$ dose/beam exposure, the corresponding $CH_3$ adsorption starts to exhibit saturation, within the present experimental dose/exposure range. This seems to be the general trend for all the incident energies considered. Cl exhibits higher coverage as compared to $CH_3$ coverage (also cf., Supplementary Data 5: Fig. 5S). As mentioned earlier, dissociative adsorption of $CH_3Cl$ occurs (cf., e.g., [15]) on copper oxide surfaces, whereas $CH_3Cl$ dissociation, $CH_3$ abstraction, and Cl adsorption occur on pure Cu surfaces [14]. All of these results seem to hint at two competing (incident energy-dependent) reaction paths: One where dissociative adsorption dominates (cf., e.g., [15]), and another where only Cl adsorbs (cf., e.g., [14]). Also, note the clear enhancement of the corresponding Cl uptake curve for $E_i = 1.2$ eV.

To analyze the uptake curves, we construct reaction rate equations (slope of the uptake curves, Fig. 3) (1) and (2):

$$\frac{dN_{CH_3}\theta_{CH_3}}{dt} = F\alpha\left(1-\theta_{CH_3}\right)\left(1-\theta_{Cl}\right), \tag{1}$$

$$\frac{dN_{Cl}\theta_{Cl}}{dt} = F\alpha\left(1-\theta_{CH_3}\right)\left(1-\theta_{Cl}\right) + F\beta\left(1-\theta_{Cl}\right) - k_d {N_{Cl}}^2 \theta_{Cl}^2, \tag{2}$$

based on the simple reaction mechanisms depicted in Fig. 4. As mentioned earlier, two different competing reaction pathways seem to contribute to the resulting uptake curves, viz., Reaction I: both dissociated $CH_3$ and Cl adsorb on the surface, and Reaction II: dominant Cl adsorption (cf., possible electron attachment mechanism in Supplementary Data 4: Fig. 4S). Which reaction (I or II) dominates depends on the incident energy (*vide ante*). In addition, Reaction III: associative desorption of Cl may also occur in the exposure region (for the conditions) with a Cl coverage smaller than $CH_3$ coverage (see Supplementary Data 5: Fig. 5S (a)-(c)). (We observed no significant changes in the O-1*s* areal intensity from the XPS spectra of the flat $Cu_2O(111)$, before and after energetic $CH_3Cl$ dosage.)

In Eqs. (1) and (2), $N_{CH_3}$ and $N_{Cl}$ give the areal densities of the possible adsorption sites for $CH_3$ and Cl on the $Cu_2O(111)$ surface,

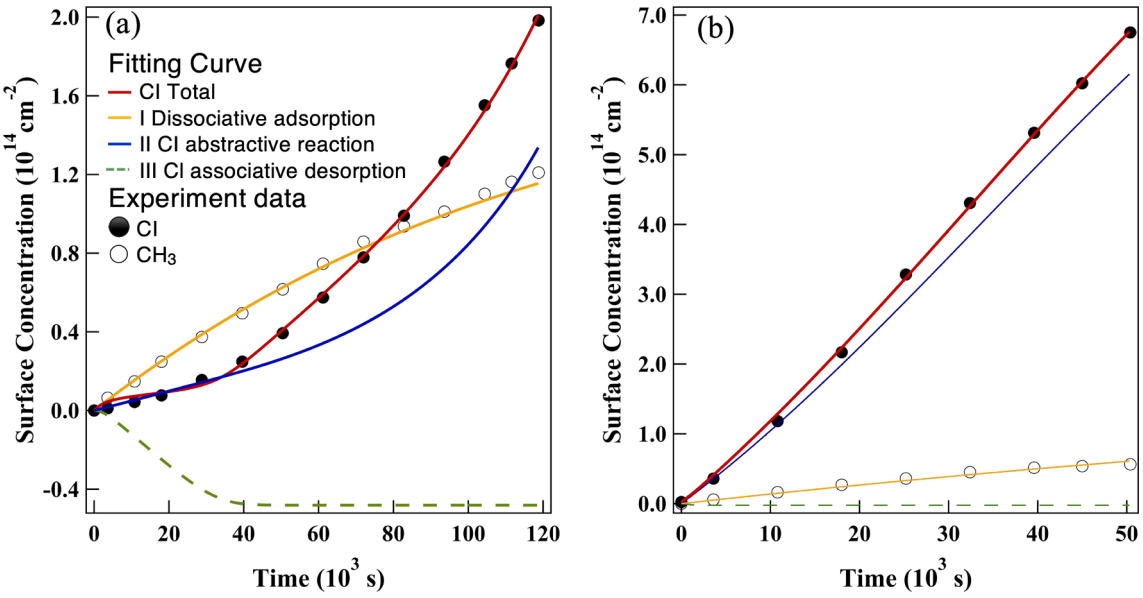


**Fig. 5.** Experimental uptake curve and fitting curve (a) 0.7 eV, (b) 1.2 eV with Equations (1) and (2).

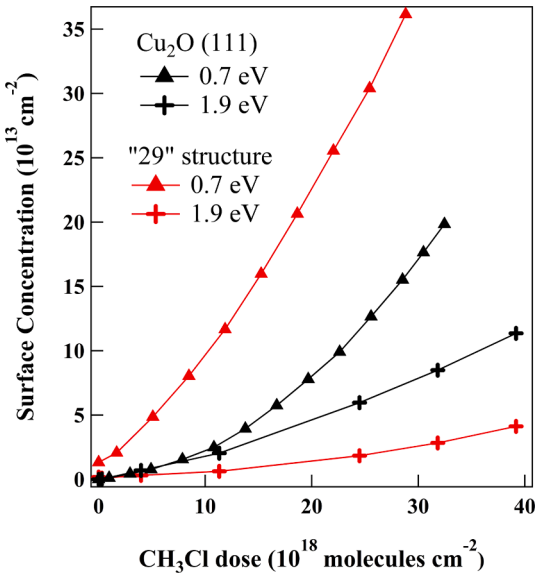


**Fig. 6.** Cl uptake curves for $CH_3Cl$ incident at various translational energies on $Cu_2O(111)$ and the bulk $Cu_2O$ precursor "29"-structure on Cu(111).

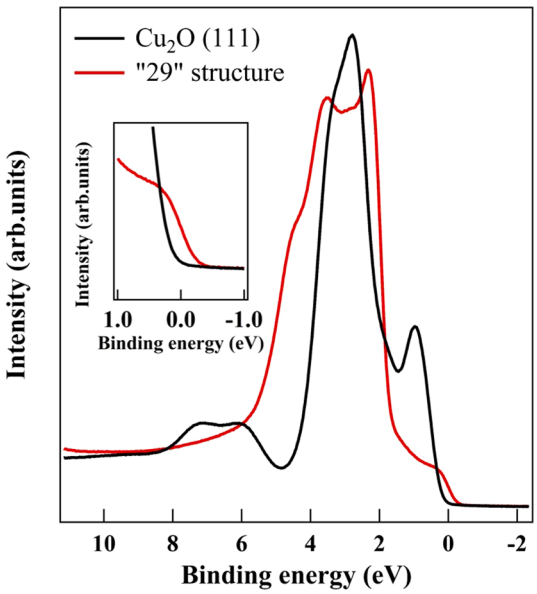


**Fig. 7.** Comparison of the valence band of $Cu_2O(111)$ and the "29" structure.

respectively. $\theta_{CH_3}$ and $\theta_{Cl}$ give the coverages, defined as the ratio of the number of adsorbates to that of possible adsorption sites for $CH_3$ and Cl on the $Cu_2O(111)$ surface, respectively. We expressed the reaction rates in terms of the flux density $F$ of incident molecular beam, the reaction probability $\alpha$ of Reaction I, the reaction rate constant $\beta(\theta_{Cl})$ for Reaction II, and the Cl associative desorption rate constant $k_d$ $(\theta_{Cl})$ for Reaction III.

The first terms on the right-hand sides of Eqs. (1) and (2) represent Reaction I in Fig. 4. The second and third terms in Eq. (2) represent Reaction II and Reaction III in Fig. 4, respectively. Fitting results using equations (1) and (2) are shown in Fig. 5 for 0.7 and 1.2 eV $CH_3Cl$ incidence on $Cu_2O(111)$ (cf., Supplementary Data 5: Fig. 5S with the parameters in Supplementary Data 5: Table 1S). Although simple, the reaction models depicted in Fig. 4 reproduce the experimental uptake curves for $CH_3$ and Cl quite well. The slope of the uptake curve corresponds to the beam-exposure dependence of reaction rate. In Fig. 3, we see that the $CH_3$ adsorption rate decreases with increasing $CH_3Cl$ exposure, while the Cl adsorption rate increases (in general). The Cl adsorption may accelerate with further Cl adsorption. We again note the predominantly large and increasing Cl reaction rate at $E_i = 1.2$ eV as compared to the correspondingly reduced and decreasing $CH_3$ reaction rate (at the same energy).

The relative importance of Reactions I and II depends on the $CH_3Cl$ incident energy and Cl coverage (cf., Fig. 5, Supplementary Data 4 and 5: Fig. 4S and Fig. 5S). Comparing Fig. 5(a) and (b), we see that Reaction I dominates at (low) incident energy 0.7 eV, and Reaction II dominates at (high) incident energy 1.2 eV. We also see from Fig. 5(a) that the Cl adsorption in Reaction II increases with Cl coverage.

Next, in Fig. 6, we compare the reaction of $CH_3Cl$ on the surface of bulk Cu oxide and on a very thin oxide layer grown on Cu(111), viz., the bulk $Cu_2O$ precursor "29"-structure on Cu(111) [20] at $T_S = 300$ K. We see that reaction occurs more efficiently on the "29"- structure when compared at $E_i = 0.7$ eV. This may be due to the difference in available adsorption sites for Cl and/or the contribution of Reaction II, with

predominant Cl adsorption (cf., difference in densities of states at the Fermi level, Binding energy = 0 eV in Fig. 7). At $E_i = 1.9$ eV, Reaction II, with predominant Cl adsorption (cf., Supplementary Data 4: Fig. 4S), the "29"-structure exhibits less reactivity possibly due to the smaller density of states just below the Fermi level (cf., Binding energy > 0 eV, Fig. 7).

## 4. Summary

To examine the elementary steps in the Rochow-Müller process, we subjected copper oxides, viz., $Cu_2O(111)$ and the bulk $Cu_2O$ precursor "29"-structure on Cu(111), to supersonic (0.5–1.9 eV) molecular beams (SSMB) of $CH_3Cl$. We then peformed X-ray photoemission spectroscopy (XPS) in conjunction with synchrotron radiation (SR) to determined the corresponding adsorbed species present. We identified Cl as the prevailing adsorbed species (higher than that of adsorbed carbonaceous species) coming from $CH_3Cl$ dissociation. We also identified two competing adsorption processes, with one dominating over the other depending on the incident energy. Comparison of the bulk $Cu_2O$ and the "29"-structure suggests the possible efficacy of thin oxide films as catalysts working at low temperatures. We will further consider the effects of surface temperature in a future study.

## CRediT authorship contribution statement

**Koki Hayashida:** Writing – review & editing, Writing – original draft, Investigation, Formal analysis, Data curation. **Yasutaka Tsuda:** Writing – review & editing, Formal analysis, Data curation. **Natsumi Murase:** Formal analysis, Data curation. **Takashi Yamada:** Writing – review & editing, Investigation, Formal analysis, Data curation. **Akitaka Yoshigoe:** Writing – review & editing, Methodology. **Wilson Agerico Diño:** Writing – review & editing, Writing – original draft, Investigation. **Michio Okada:** Writing – review & editing, Writing – original draft, Supervision, Resources, Project administration, Methodology, Investigation, Funding acquisition, Formal analysis, Data curation, Conceptualization.

## Declaration of competing interest

The authors declare that they have no known competing financial interests or personal relationships that could have appeared to influence the work reported in this paper.

## Data availability

Data will be made available on request.

## Acknowledgements

The authors thank MEXT (Ministry of Education, Culture, Sports, Science and Technology-Japan) for Grants-in-Aid for Scientific Research (JP20K21171, JP15KT0062, JP26248006, JP20H02638). They are also thankful for the assistance by Yauka Hashimoto, Tetsuya Sakamoto, Naoyuki Shimode, Shizuka Nishi, Hikaru Yoshida, and all of the staff at BL23SU in SPring-8. The synchrotron radiation experiments were performed at BL23SU in SPring-8, with the approval of the Japan Synchrotron Radiation Research Institute (JASRI) and Japan Atomic Energy Agency (JAEA) (Proposal Nos. 2023B3801, 2023A3801,2022B3801, 2022A3801, 2021B3801, 2021A3801, 2020B3801, 2020A3801, 2019B3801, 2019A3831, 2019A3801, 2018B3831, 2018B3801, 2018A3831, 2018A3801, 2017B3801, 2017A3801). This work was performed under the Shared Use Program of JAEA Facilities (Proposal Nos. 2019A-E13, 2018B-E12, 2018A-E17) with the approval of Nanotechnology Platform project supported by MEXT. This work was also financially supported by Shin-Etsu Chemical Co., Ltd., Japan.

## Appendix A. Supplementary data

Supplementary data to this article can be found online at https://doi.org/10.1016/j.apsusc.2024.160475.

## References

[1] E.G. Rochow, The direct synthesis of organosilicon compounds, J. Am. Chem. Soc. 67 (1945) 963–965, https://doi.org/10.1021/ja01222a026.
[2] R. Müller, One hundred years of organosilicon chemistry, J. Chem. Edu. 42 (1965) 41–47, https://doi.org/10.1021/ed042p41.
[3] D. Seyferth, Dimethyldichlorosilane and the direct synthesis of methylchlorosilanes, The Key to the Silicones Industry, Organometallics. 20 (2001) 4978–4992, https://doi.org/10.1021/om0109051.
[4] Y. Zhang, J. Li, H. Liu, Y. Ji, Z. Zhong, F. Su, Recent advances in Rochow-Müller process research: driving to molecular catalysis and to a more sustainable silicone industry, ChemCatChem 11 (2019) 2757–2779, https://doi.org/10.1002/cctc.201900385.
[5] A. Woelke, S. Imanaka, S. Watanabe, S. Goto, M. Hashinokuchi, M. Okada, T. Kasai, Dissociative adsorption of methyl chloride on Si(001) studied by scanning tunneling microscopy, J. Electron Microsc. (tokyo) 54 (Suppl 1) (2005) i21–i24, https://doi.org/10.1093/jmicro/54.suppl_1.i21.
[6] M. Okada, S. Goto, T. Kasai, Dynamical steric effect in the decomposition of methyl chloride on a silicon surface, Phys. Rev. Lett. 95 (2005) 176103, https://doi.org/10.1103/PhysRevLett.95.176103.
[7] M. Okada, S. Goto, T. Kasai, Reaction-path selection with molecular orientation of $CH_3Cl$ on Si{100}, J. Am. Chem. Soc. 129 (2007) 10052–10053, https://doi.org/10.1021/ja070931b.
[8] M. Okada, S. Goto, T. Kasai, Steric effects in dissociative adsorption of low-energy $CH_3Cl$ on Si(100): Orientation and steering effects, J. Phys. Chem. C Nanomater. Interfaces. 112 (2008) 19612–19615, https://doi.org/10.1021/jp807052s.
[9] H. Ito, M. Okada, D. Yamazaki, T. Kasai, Steric effects in the scattering of oriented $CH_3Cl$ molecular beam from a Si(111) surface, J. Phys. Chem. A. 114 (2010) 3080–3086, https://doi.org/10.1021/jp907225b.
[10] M. Okada, Surface chemical reactions induced by well-controlled molecular beams: translational energy and molecular orientation control, J. Phys. Condens. Matter. 22 (2010) 263003, https://doi.org/10.1088/0953-8984/22/26/263003.
[11] M. Okada, Supersonic molecular beam experiments on surface chemical reactions, Chem. Rec. 14 (2014) 775–790, https://doi.org/10.1002/tcr.201402003.
[12] T. Makino, S. Zulaehah, J.S. Gueriba, W.A. Diño, M. Okada, $CH_3Cl$/Cu(410): interaction and adsorption geometry, J. Phys. Chem. C. 122 (2018) 11825–11831, https://doi.org/10.1021/acs.jpcc.8b01296.
[13] K. Takeyasu, M. Okada, Adsorption geometry of methyl chloride weakly interacting with Ag(111), J. Phys. Commun. 2 (2018) 075017, https://doi.org/10.1088/2399-6528/aad1d0.
[14] T. Makino, Y. Tsuda, A. Yoshigoe, W.A. Diño, M. Okada, $CH_3Cl$ dissociation, $CH_3$ abstraction, and Cl adsorption from the dissociative scattering of supersonic $CH_3Cl$ on Cu(111) and Cu(410), Applied Surf. Sci. 642 (2024) 158568, https://doi.org/10.1016/j.apsusc.2023.158568.
[15] J. Li, L. Yin, Y. Ji, H. Liu, Y. Zhang, X. Gong, Z. Zhong, F. Su, Impact of the $Cu_2O$ microcrystal planes on active phase formation in the Rochow reaction and an experimental and theoretical understanding of the reaction mechanism, J. Catalysis 361 (2018) 73, https://doi.org/10.1016/j.jcat.2018.02.010.
[16] F. Tang, J. Li, Y. Zhu, Y. Ji, H. Li, H. Liu, X. Wang, Z. Zhong, F. Su, In situ generating $Cu_2O$/Cu heterointerfaces on the $Cu_2O$ cube surface to enhance interface charge transfer for the Rochow reaction, Catal. Sci. Technol. 11 (2021) 2202, https://doi.org/10.1039/d0cy02015j.
[17] J. Li, Z. Zhang, Y. Ji, Z. Jin, S. Zou, Z. Zhong, F. Su, One-dimensional Cu-based catalysts with layered Cu–$Cu_2O$–CuO walls for the Rochow reaction, Nano Res. 9 (2016) 1377, https://doi.org/10.1007/s12274-016-1033-x.
[18] S. Liu, Y. Wang, Y. Zhu, G. Wang, Z. Zhang, H. Che, L. Jia, F. Su, Controllably oxidized copper flakes as multicomponent copper-based catalysts for the Rochow reaction, RSC. Adv. 4 (2014) 7826, https://doi.org/10.1039/C3RA46970K.
[19] W. Liu, L. Jia, Y. Wang, L. Song, Y. Zhu, X. Chen, Z. Zhong, F. Su, Partially reduced CuO nanoparticles as multicomponent Cu-based catalysts for the rochow reaction, Ind. Eng. Chem. Res. 52 (2013) 6662, https://doi.org/10.1021/ie400369z.
[20] K. Hayashida, Y. Tsuda, T. Yamada, A. Yoshigoe, M. Okada, Revisit of XPS studies of supersonic $O_2$ molecular adsorption on Cu(111): copper oxides, ACS Omega 6 (2021) 26814, https://doi.org/10.1021/acsomega.1c04663.
[21] Y. Tsuda, K. Oka, T. Makino, M. Okada, W.A. Diño, M. Hashinokuchi, A. Yoshigoe, Y. Teraoka, H. Kasai, Initial stages of $Cu_3Au(111)$ oxidation: oxygen induced Cu segregation and the protective Au layer profile, Phys. Chem. Chem. Phys. 16 (2014) 3815, https://doi.org/10.1039/C3CP54709D.
[22] K. Oka, Y. Tsuda, T. Makino, M. Okada, M. Hashinokuchi, A. Yoshigoe, Y. Teraoka, H. Kasai, The effects of alloying and segregation for the reactivity and diffusion of oxygen on $Cu_3Au(111)$, Phys. Chem. Chem. Phys. 16 (2014) 19702, https://doi.org/10.1039/C4CP02675F.
[23] Y. Tsuda, A. Yoshigoe, Y. Teraoka, M. Okada, Surface temperature dependence of oxidation of $Cu_3Au(111)$ by an energetic oxygen molecule, Mater. Res. Express 3 (2016) 035014, https://doi.org/10.1088/2053-1591/3/3/035014.
[24] M. Okada, Y. Tsuda, K. Oka, K. Kojima, W.A. Diño, A. Yoshigoe, H. Kasai, Experimental and theoretical studies on oxidation of Cu-Au alloy surfaces: effect of

bulk Au concentration, Sci. Rep. 6 (2016) 31101, https://doi.org/10.1038/srep31101.
[25] Y. Tsuda, J.S. Gueriba, T. Makino, W.A. Diño, A. Yoshigoe, M. Okada, Interface atom mobility and charge transfer effects on CuO and $Cu_2O$ formation on $Cu_3Pd$ (111) and $Cu_3Pt$(111), Sci. Rep. 11 (2021) 3906, https://doi.org/10.1038/s41598-021-82180-w.
[26] D.A. Shirley, High-resolution X-ray photoemission spectrum of the valence bands of gold, Phys. Rev. B 5 (1972) 4709–4714, https://doi.org/10.1103/physrevb.5.4709.